

# Wave Characterization for the Diagnosis of Semi-Submerged Structures

A. B. Coli<sup>†</sup>; J. A. Santos<sup>‡</sup> and R. Capitão<sup>§</sup>

DHA-NPE

LNEC, Lisbon,

1700-066, Portugal

<sup>†</sup> abcoli@lnec.pt <sup>‡</sup> jasantos@lnec.pt <sup>§</sup> rcapitao@lnec.pt



## ABSTRACT

COLI, A. B.; SANTOS, J. A. and CAPITÃO, R., 2006. Wave characterization for the diagnosis of semi-submerged structures. Journal of Coastal Research, SI 39 (Proceedings of the 8th International Coastal Symposium), 1468 - 1473. Itajaí, SC, Brazil, ISSN 0749-0208.

In order to assess the number of days per year an autonomous vehicle carrying a device to survey the envelope of the armour layer of rubble-mound breakwaters can sail close to the Sines' west breakwater, a general observed wave regime was established at a point in front of the breakwater, over depth contour -35.7 m CD. For this, the relevant sea state parameters of 13463 wave records measured at the SINES 1D directional wave buoy were transferred to that point by linear interpolation of the results obtained in a transfer matrix between the measuring point and the point in front of the breakwater. This transfer matrix, specially created for this study, was defined by using the SWAN model for wave propagation assuming that the sea states could be characterized by a JONSWAP spectrum. The SWAN model and the nested grid scheme adopted proved adequate for this region. The results clearly show the influence of wave refraction on the sea states transferred to the point close to the breakwater. Assuming that the operational wave height limit of the autonomous vehicle is a significant wave height of 1.0 m, then from the general observed regime close to the breakwater it may be concluded that the vehicle can operate in 27% of the time.

**ADDITIONAL INDEX WORDS:** *General observed wave regime, transfer of wave regimes, sines' west breakwater, SWAN model.*

## INTRODUCTION

Rubble-mound breakwaters are designed under the proviso that maintenance and repair works are going to be needed during the structure's life. However, the continuous monitoring of any given stretch of this kind of structures is not feasible yet. This implies that the most common monitoring procedure so far is the periodic inspection, which, in most cases, has been limited to the inspection of the emerged part only, due to the cost of underwater inspection.

In Portugal, the National Civil Engineering Laboratory (LNEC) is responsible for the inspection on the rubble mound breakwaters that protect the ports controlled by the Portuguese Port Directorate (which leaves out the major independent ports: Leixões, Aveiro, Lisboa, Setúbal and Sines).

This work started in 1985 and has been limited to the periodic inspection of the above water part of those breakwaters. The information gathered in these inspections is stored in a database that can be queried to produce reports on both the structure's status at the time of any inspection and the evolution of the structure's damages between inspections. Based on this information it is possible to give some hints on the expected evolution of the structure, thus helping in the decision process related to maintenance or repair works to be carried out on the structure.

In spite of the availability of sea wave data collected at wave buoys deployed at some points of the Portuguese coast, those prognostics on the structure's evolution are seldom based on the wave regime measured or estimated at the structure's location. Another point deserving improvement is the quantification of the changes in the armour layer geometry, something that can be accomplished by means of the survey of the armour layer envelope. LNEC is involved, together with the Institute for Systems and Robotics of Lisbon's Technical University (ISR) and the Port of Sines Authority (APS) in a joint research project, code named MEDIRES, which aims at developing a device able to produce efficient and accurate surveys of both the emerged and submerged parts of the armor layer of rubble-mound breakwaters.

This device is to be made of a mechanically scanned sonar

profiler to survey the submerged part of the structure, and of a laser range finder to survey the emerged part of the structure. This device is then deployed on an autonomous surface vehicle whose navigation and control systems ensure the maneuver repeatability and hence the quality of the collected data, Figure 1.

For a given stretch of the structure, once the envelope of the armour layer is surveyed, one can establish the probability of failure of that stretch if the failure mode function is known and the probability distributions of both the resistance and loads variables are known. For rubble-mound breakwaters, the failure mode that interests most is the hydraulic stability of the armour layer.

The most important load variable for this kind of structures is the sea wave height. This means that in order to evaluate the probability of failure of the surveyed armour layer, one has to establish the wave regime close to the structure. That is why one of the MEDIRES tasks is the development of a tool that is able to transfer the offshore sea wave characteristics to a point close to the structure's site. The offshore wave characteristics, such as

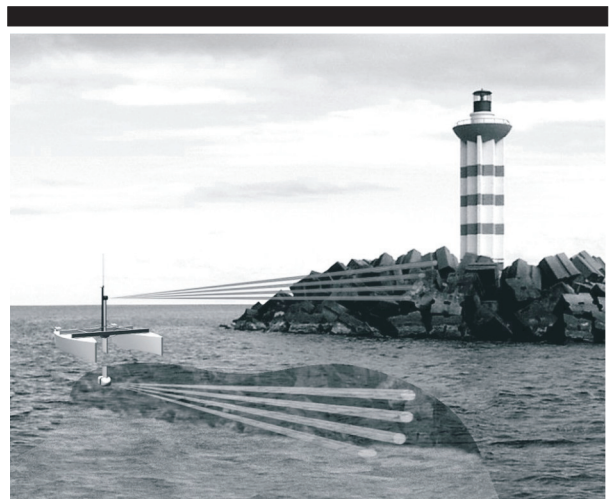


Figure 1. The surveying device and the autonomous vehicle.

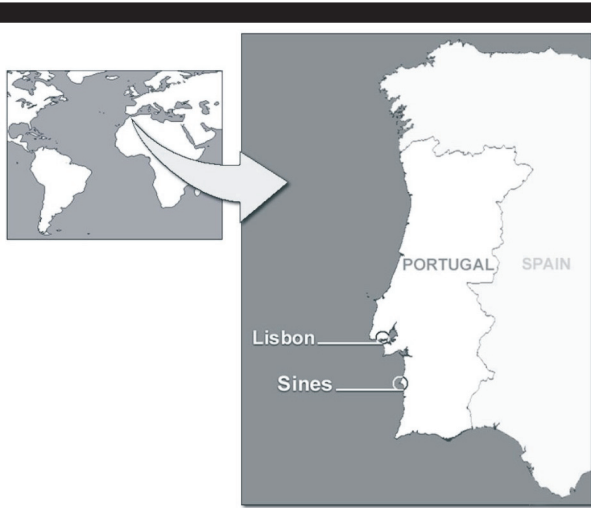


Figure 2. Location of Portugal and Sines.

the significant wave height, peak period and direction, can be obtained from a pitch-and-roll buoy or from the results in a node of a large scale numeric wave model. The transfer of these parameters to the vicinity of the structure can be useful for

- 1) issuing warnings related to the safety of the breakwater, the port facilities and the terminal operations;
- 2) together with the armor layer surveys, establishing the structure's response to storm episodes;
- 3) characterizing the general and extreme wave regimes that will enable the prediction on the structure's evolution;
- 4) establishing the timing for the structure's maintenance and repair works, as well as for the inspections themselves.

The methodology and the tools to be developed within the scope of the MEDIRES project are to be tested at the west breakwater of the Sines port. This port is located in the southwestern part of Portugal, about 100 km south of Lisbon (Figure 2). It is an open coast port and it is one of the few deep water European ports. It is mainly a port for bulk products, namely, oil, oil products and coal. The oil and the oil products terminals are protected by the west breakwater, which has a length of 2200 m and whose armour layer is made of Antifer cubes weighting 90 ton.

This paper presents the characterization of the sea wave regimes at both the wave buoy deployed close to Sines, the so-called SINES 1D buoy, and the region in front of the west breakwater. Since there are no wave data collected close to the

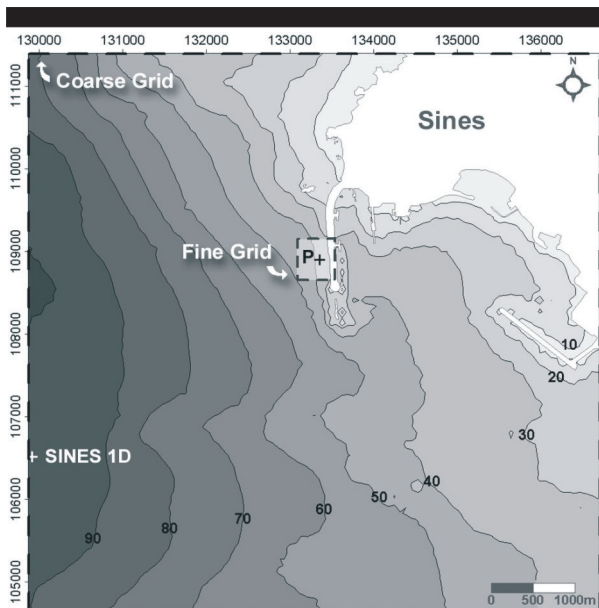


Figure 3. The maritime region close to Sines' west breakwater and the spatial grids employed in this study.

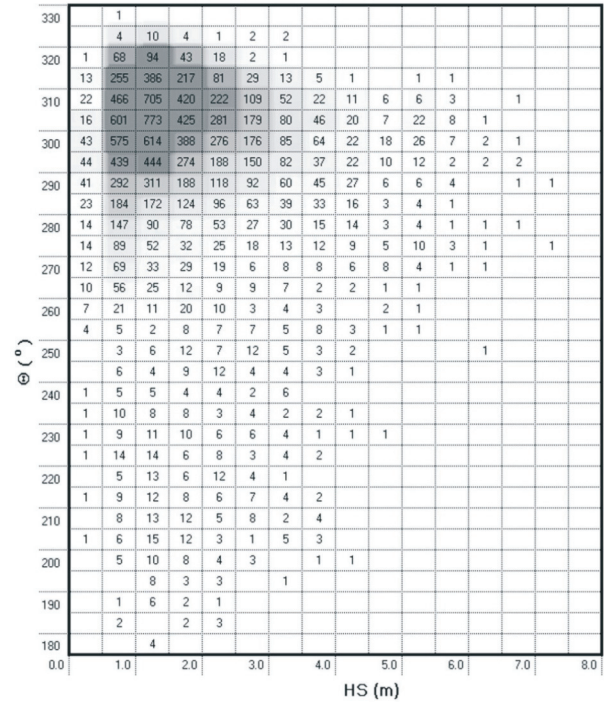


Figure 4. General observed wave regime at the Sines 1D buoy in terms of number of occurrences.

breakwater, there is the need to transfer to that region the wave regime defined at the location of the SINES 1D buoy.

The work focuses on the general observed wave regime whose definition enables the evaluation of the annual number of days the surveys can be carried out for the given operational constraints of the autonomous surface vehicle where the surveying device is to be deployed. The procedures for the transfer of the general observed wave regime can be easily extended to transfer the extreme wave regime, if this is available. Based on this regime one can perform the diagnosis of the surveyed structure.

After this introduction, the paper presents the basic concepts of sea wave regimes definition and of the procedures available for the transfer between two locations, which is a topic of paramount importance for this kind of study, as well as the role of the SWAN model (BOUJ *et al.*, 1996) on this transfer. Then, the general observed wave regime at the location of the SINES 1D buoy is defined and transferred to a point in front of the west breakwater. The spatial grids used with the SWAN model as well as its control parameters are also presented. After the discussion on the results obtained at the several grids employed and on the possible applications for the transfer matrix created to solve this problem, the conclusions are presented.

## BASIC CONCEPTS

### Sea Wave Regimes

In sea wave studies, two different statistical methods can be applied to the sea wave parameters: the so-called short term and long term statistics. In the short term statistics, the free-surface elevation, periods and directions of a sea wave record are described having in mind the characterization of the sea state in the time interval of a typical wave record, usually 20 minutes. Long term statistics use a characterization of sea states, along several years, to evaluate the sea wave climate. The sea wave climate, at a given point of the ocean, is defined by the long term statistical behavior of the basic parameters that can be derived from a wave record, such as significant wave height (HS), mean zero up-crossing period (TZ), peak direction ( $\Theta$ ) the mean

direction of the spectrum peak frequency) and directional spectrum [ $E(\sigma, \theta)$ ]. The wave climate is composed by a set of sub-climates, called sea wave regimes.

A sea wave regime is then basically a statistical treatment of the basic parameters of sea wave records, aiming to describe statistical characteristics of the sea wave climate that are appropriate for some specific engineering study. Thus, one can have, among others, the general observed wave regime, the average regime or the extreme wave regime.

The general observed wave regime consists in histograms, single and joint histograms of the basic wave parameters (HS, TZ,  $\Theta$ ), and possibly in time series charts of the same parameters. These may be accompanied, when possible statistically, by linear regressions which attempt to establish relationships between the parameters. The extreme wave regime consists of the extrapolated values of the annual maximum significant wave height and maximum wave height, for a set of return periods, together with associated wave periods and directions to those extrapolated values. In the design of maritime structures the two regimes are useful.

This paper aims to characterize the general wave regime close to Sines' west breakwater. This is done by transferring, using a numerical model, the offshore general observed wave regime to the vicinity of the breakwater.

### The Transfer of Sea Wave Regimes

For the definition of a sea wave regime plenty of sea wave data should be available at the desired point. These data should ideally be measured by wave buoys deployed close to that point. When no data are available, a possible solution is to use data collected at points not too far from the desired location and to transfer those data offshore and then to the desired point. COLI *et al.* (2002) present a methodology to perform such transfer of sea wave regimes.

For the Sines' west breakwater there are no wave buoy data collected in the vicinity of the structure but there are data collected by a pitch and roll buoy (Wavec/Direc) deployed at a point located a couple of kilometers to the west of that structure over the -97 m (CD) depth contour, Figure 3, the so-called SINES 1D buoy, for which there were 8 years of directional measurements available.

The transfer of the sea wave data was made by means of the SWAN numerical model (BOUJ *et al.*, 1996). This is a phase averaging wave model, able to characterize the sea waves in nearshore regions, up to the breaking zone.

Conceptually, the SWAN can be considered a third generation model and it is based on the equation for the conservation of wave action:

$$\frac{\partial N}{\partial t} + \frac{\partial}{\partial x}(c_x N) + \frac{\partial}{\partial y}(c_y N) + \frac{\partial}{\partial \sigma}(c_\sigma N) + \frac{\partial}{\partial \theta}(c_\theta N) = \frac{S}{\sigma} \quad (1)$$

in which  $N(\sigma, \theta, x, y, t)$  is the wave action (the quotient of the directional spectrum to the intrinsic frequency,  $\sigma$ ),  $x$  and  $y$  are the horizontal coordinates,  $\theta$  is the mean wave direction per frequency, and  $c_x$ ,  $c_y$ ,  $c_\sigma$ , and  $c_\theta$  are propagation velocities in the corresponding spaces. The term  $S = S(\sigma, \theta)$ , at the right hand side of the action balance equation, is the energy source / sink term and represents the effects of wave generation and dissipation and the non-linear wave-wave interactions.

The SWAN model has implemented the physical processes of propagation through geographic space, refraction and shoaling due to bottom and current variations, blocking and reflections by opposing currents, transmission through or blockage by obstacles and dissipation effects due to whitecapping, bottom friction and wave breaking. The propagation in the SWAN model, in both geographic and spectral spaces, is carried out by using implicit numerical schemes.

## RESULTS

### General Observed Wave Regime at SINES1D

At Sines, the directional wave data have been collected by a Wavec buoy, called SINES 1D, since May 1988. This buoy was deployed at a point whose coordinates are 37° 55' 16" N, 8° 55' 44" W, where the water depth is 97 m (CD).

The data sources for this study are the monthly and quarterly reports of processed wave data published by the Portuguese Hydrographic Institute (IH), COSTA (1988-1995). From these reports, the three-hourly values (i.e., records of twenty minutes taken every three hours) of HS, TZ and  $\Theta$  were collected and considered in this study. These parameters, from 13463 wave records ranging from May 1988 to December 1995, although with some measurement gaps, were used to produce the general wave regime at SINES 1D. Only the values taken every 3 hours were considered in this general wave regime. This means that intermediate values measured during storms (when the buoy broadcasts wave measurements continuously) were not considered and so the highest significant wave height in the built sample may not be the highest HS that occurred in that time interval.

A summary of the general observed wave regime at the SINES1D buoy is presented in Figure 4, where the bivariate histogram of HS and  $\Theta$  are presented.

The wave directions of the sea states observed at SINES 1D buoy range from 180° to 330°. The most frequent waves (occurrences above 10% in each interval) have a wave direction in the interval 295° to 315°. Significant wave heights range between 0.25 m and 7.5 m, the most frequent waves having HS values between 0.5 m and 2.5 m. Significant wave heights above 5 m are found in the direction range 250° to 320°. The observed wave peak periods (TP) at the SINES1D buoy are in the range 4 to 20 s, while the most frequent range is from 6 to 10 s. Table 1 presents the peak periods' range per direction sectors.

For the significant wave heights, the mean is 1.66 m and the standard deviation is 0.91 m and the most frequent value lies between 1.0 and 1.5 m. For the peak period, the mean and standard deviation are 9.0 s and 2.29 s, respectively, and the most frequent values lie between 7 and 8 s. For the peak direction at the location of the SINES 1D the most frequent values are contained in the interval 305°-310°.

### SWAN Model Run

The maritime region in the neighbourhood of the Sines' west breakwater presents no special features: the bottom depth contours are more or less parallel to the breakwater alignment. Close to the breakwater the sea bottom has a high slope. The spatial grid employed to characterize the sea bottom at the study region encompasses the port structures, the coastline and the location of the SINES 1D wave buoy, Figure 3. Bottom data was collected from the Portuguese nautical chart *Cabo de Sines a Lagos* (PT 324205) and from some bathymetric surveys in the vicinity of the west breakwater commissioned by the APS in 1998 and 2000.

In order to choose the most adequate spatial grid, some tests were conducted to assess the accuracy of the grid and the CPU-time needed. The solution adopted consists of two quadrangular grids, one covering the Sines region, with a coarse grid, and a nested, finer, grid that covers the area close to the breakwater.

Both grids are presented in Figure 3. The coarse grid covers the whole area presented in that figure whose boundaries are the

Table 1. SINES1D buoy TP ranges by directional sectors.

| Sector | TP min (s) | TP max (s) | Occurrence (%) |
|--------|------------|------------|----------------|
| SSW    | 4          | 13         | 1.05           |
| SW     | 5          | 14         | 1.60           |
| WSW    | 4          | 13         | 1.40           |
| W      | 4          | 20         | 6.5            |
| WNW    | 4          | 20         | 43.26          |
| NW     | 4          | 18         | 46.02          |

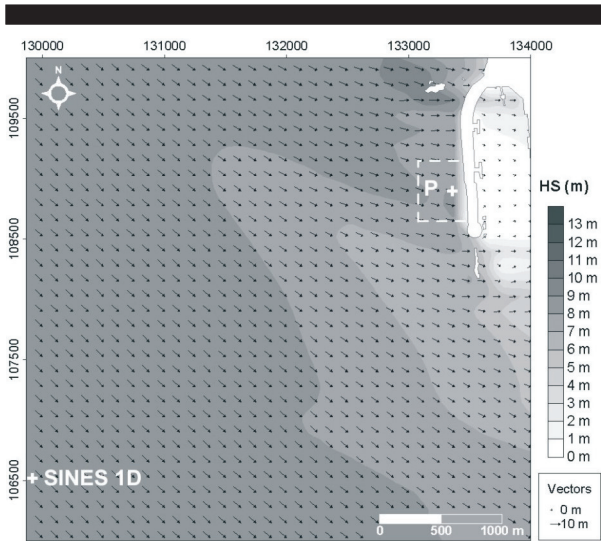


Figure 5. Example of a SWAN run for a sea state with HS = 9 m, TP = 18 s and  $\Theta = 315^\circ$ .

meridians  $8^\circ 51' 15.4''$  W and  $8^\circ 55' 52.6''$  W and the parallels  $37^\circ 54' 18.2''$  N and  $37^\circ 57' 58.9''$  N. The width of this coarse grid is 6875 m and the height is 6750 m, the size of the side of the quadrangular grid units being 125 m. The location of the SINES 1D buoy is close to the western domain boundary. The fine grid has a resolution of 5 m, a width of 450 m and a height of 500 m. Point P, near the Sines' west breakwater, has the coordinates  $8^\circ 53' 31.57''$  W and  $37^\circ 56' 36.98''$  N, and is over a water depth of 35.7 m (CD). In all the computations, the tide level considered was the mean annual value of 3.3 m.

The wave parameters needed to run the SWAN model were introduced at the coarse grid boundary. Since the number of sea wave data records available is quite high (13463), it was decided that, instead of running the SWAN model for each of those records individually, the transfer function between the wave buoy location and a point in front of the west breakwater should be evaluated for a 3-D matrix covering the range of possible values for the wave height, period and direction at the buoy. This procedure reduces substantially the number of

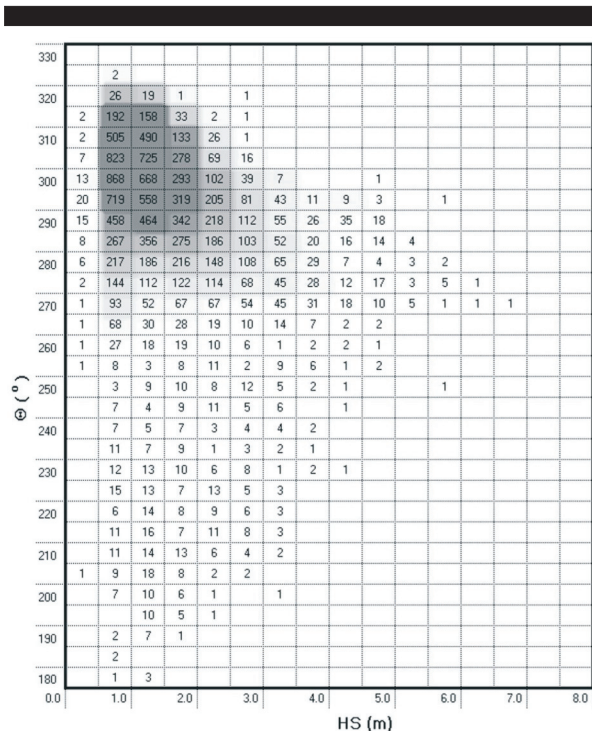


Figure 6. General wave regime at a point P near Sines' west breakwater in terms of number of occurrences.

Table 2. TP ranges by directional sectors at point P.

| Sector | TP min (s) | TP max (s) | Occurrence (%) |
|--------|------------|------------|----------------|
| SSW    | 4          | 11         | 0.94           |
| SW     | 5          | 14         | 1.74           |
| WSW    | 4          | 12         | 1.43           |
| W      | 4          | 20         | 12.23          |
| WNW    | 4          | 17         | 53.98          |
| NW     | 4          | 11         | 29.61          |

computations and enables also the transfer, in real time, to a point close to the breakwater of the characteristics of the sea waves measured at the buoy.

Since there were no spectral data available at the time of performing this study, the wave data supplied to the model were the result of a parameterisation of the spectrum measured at the buoy location. Thus, for each set of HS, TP and  $\Theta$  values a directional wave spectrum was defined at the boundary of the coarse grid as the product of a JONSWAP spectrum, with a peak enhancement factor of 3.3, by a directional spreading function of cosine-type to an even power (2s), s being equal to 10. The frequency discretization used 31 frequencies ranging from 0.02 to 0.4 Hz, with a logarithmic distribution. The directional discretization covered a range of  $180^\circ$  with a  $2^\circ$  resolution.

All the computations, with SWAN version 40.11, cycle III, were carried out in stationary mode, with no tidal currents or wind blowing over the study region. In the operation of the SWAN model the following phenomena were included: refraction, shoaling and dissipation by whitecapping, bottom friction and depth-induced wave breaking. Each run of the SWAN model was made of two steps. In the first step the model was run with the JONSWAP spectrum parameterisation at the boundary of the coarse grid. The JONSWAP spectra were defined at the same boundary of the peak direction, if it is N, S or W, and at two boundaries if the peak direction is from the other octants; for example, to  $\Theta = SW$ , the spectra are defined at S and W boundaries. These runs produced the wave spectra along the boundary of the fine nested grid, which were the boundary conditions needed for running the second step, now at the nested grid.

The results of the SWAN model, in every point of the domain, consisted in the significant wave height (HS), the mean and the peak period (TZ, TP), the mean and the peak wave direction ( $\Theta$  m,  $\Theta$ ), a directional spreading (dspr) and a water level ( $\eta$ ).

Figure 5 shows the SWAN results obtained for a sea state with HS = 9.0 m, TP = 18 s and  $\Theta = 315^\circ$  (SW).

### General Wave Regime Close to the West Breakwater

To carry out the transfer to point P of the 13463 three-hourly values of parameters measured at SINES 1D, the transfer matrix created for this task had to be interpolated to those values. In order to make the interpolations easier, it was decided to have constant intervals in the three parameters of the transfer matrix. Thus, the HS input values had 1 m resolution, TP had 1 s and  $\Theta$  had  $22.5^\circ$ . The range of the offshore parameters of this transfer matrix were defined having in mind both the ranges of those parameters observed in the data measured at the SINES 1D buoy available for this study and the physically sound combinations of those parameters. For example, it would be useless to combine large significant wave heights with small peak periods, for instance HS = 4 m and TP = 4 s. For each set (HS, TP and  $\Theta$ ) at the buoy, a similar set was evaluated at the point close to the breakwater. Given the measured values at the SINES 1D buoy, the corresponding values close to the breakwater were evaluated by linear interpolation. This implied the selection of the eight points in the (HS, TP and  $\Theta$ ) space closest to the measured point.

The general wave regime resulting from these calculations has peak directions ranging from  $180^\circ$  to  $325^\circ$ , significant wave

heights from 0.25 to 7.0 m and peak periods from 4 to 20 s, see Figure 6 and Table 2. The most frequent HS (occurrences above 10% in each interval) are between 0.5 and 2.0 m while the most frequent  $\Theta$  are within 285° to 310° interval and TP between 6 and 11 s. The highest HS values (above 5 m) are found in the 270-295° direction intervals, plus the 250-255° interval, where these highest waves have TP above 11.5 s. Table 2 indicates the range of the peak periods distributed by direction sectors.

The mean and standard deviation for HS are 1.46 m and 0.69 m and, for TP, are 8.9 s and 1.71 s, respectively. The mode for HS is the 0.5-1.0 m interval, for TP is the 7-8 s interval and for  $\Theta$  is both the 295-300° and 300-305° intervals.

## DISCUSSIONS

### SWAN Modeling and Wave Data Transfer

The results of the SWAN model for the transfer matrix showed no major differences in the parameters HS, TP and  $\Theta$  at the point P calculated using either the coarse grid only or the finer grid nested on the coarse grid. The only exceptions are the sea states whose direction at the SINES 1D buoy is 180° (waves coming from south). In fact, for all the wave directions at the buoy, the TP values obtained at the point P with the coarse grid do coincide with the values obtained with the fine grid.

Apart from the south sea states, something similar happens with the HS and  $\Theta$  results, although in these cases some differences can be found between the results from the coarse and the fine grids: a maximum difference of 10% in the HS results and a maximum difference of 6° in the  $\Theta$  results can be observed.

Sea states coming from south were those where the largest differences between the results from the coarse and the fine grid were found. This fact can be seen in Figure 7, which presents the evolution of HS and  $\Theta$  at point P, for several values of TP and for sea states from south and significant wave height equal to 1 m at the buoy location. Apparently, for the coarse grid, the SWAN model was insensitive to the bathymetry close to the breakwater. For the fine grid, the bottom depth was discretized with more detail and so the depth variations could be felt by the propagating sea states and refraction that occurred.

Figure 7 shows that the difference between  $\Theta$  values obtained both with the coarse grid and the fine grid reaches the maximum of 18° at TP=11 s. In what concerns HS, the maximum difference occurs for TP=9 s and is equal to 30% of the HS value obtained with the fine grid.

### General Wave Regime

It should be noted that all the computations were made assuming that the sea states at the buoy location could be modeled by a JONSWAP spectrum whose peak period and significant wave height are given by the corresponding parameters taken from the measured wave records. In what concerns the directional spreading of the wave spectrum, it was assumed that the mean direction of the peak period obtained from the wave records is valid for all the frequencies considered in the spectrum discretization. In addition, the same directional spreading function, cosine to an even power, is used for all frequencies. These assumptions may be questionable since SOARES *et al.* (1992) found that 24% of the spectra measured at Sines were bimodal, although 63% were one-peaked spectra. Moreover, it should be pointed out that all SWAN runs were performed for a constant tide level without considering the effects of wind.

Despite these limitations, the results are an important step towards the knowledge of the general observed wave regime close to the Sines' west breakwater. By comparing the general observed wave regime measured at the SINES 1D, Figure 4, and the regime transferred to point P (close to Sines' west breakwater), Figure 6, it may be concluded that there are no major differences between the corresponding bivariate (HS,  $\Theta$ ) histograms for  $\Theta$  less than 270° (waves coming from the south

to west sector). The same does not apply for  $\Theta$  greater than 270° (waves from the west to north sector) since in this case the bivariate histogram is strongly modified from the buoy location to point P. This is an interesting result because the west breakwater has an almost north-south alignment, (Figure 3), and there are no obstacles between the domain boundaries and point P. This means that the waves that reach the wave buoy should certainly reach point P. However, only waves coming from the west to north sector experience noticeable modifications. This is due to the refraction caused by the bottom configuration, which changes the wave directions in spite of the point P being located over a water depth that is often considered not so shallow. This conclusion is confirmed with the results of Table 1 and Table 2, which show a concentration in point P of the large period waves around the west octant. In fact, the maximum value of TP=20 s observed at the buoy in the NW octant was replaced by a smaller value, TP=11 s, at point P.

## CONCLUSIONS

This paper focused on one of the several roles that the characterization of wave regimes may play in the diagnosis of semi-submerged structures: the assessment of the number of days per year the inspection activities can be carried out due to the operational constraints of the vessel that carries the instrument to survey the envelope of the armour layer of rubble-mound breakwaters. This implied the establishment of the general observed wave regime at point P, in front of the breakwater, over depth contour -35.7 m CD.

For this, the sea state parameters of the 13463 wave records measured at the SINES 1D directional wave buoy were transferred to that point by linear interpolation of the results obtained in a transfer matrix between those two points. This transfer matrix was defined by using the SWAN model for wave propagation assuming that the sea states at the buoy location could be modeled by a JONSWAP spectrum and a directional spreading function. All the SWAN runs were performed for a constant tide level and without considering wind effects.

The results clearly show the influence of wave refraction on the sea states transferred to the point close to the breakwater. In fact, for sea states coming from south to west, which are more orthogonal to the bottom depth contours, there are no major differences between the general observed wave regime bivariate histograms obtained at the SINES 1D buoy and at point P. The same does not apply for sea states coming from the west to north sector, which are more oblique to the bottom depth contours. The distribution of the period ranges per wave direction at the point close to the breakwater shows a concentration of the large periods around the west octant.

Assuming that the operational wave height limit of the autonomous vehicle is a significant wave height of 1.0 m, then from the general observed regime close to the breakwater it may be concluded that the vehicle can operate in 27% of the time.

Despite the limitations mentioned previously, the implementation of the SWAN model for the maritime region close to Sines constituted an important step towards the definition of the general observed wave regime in this region.

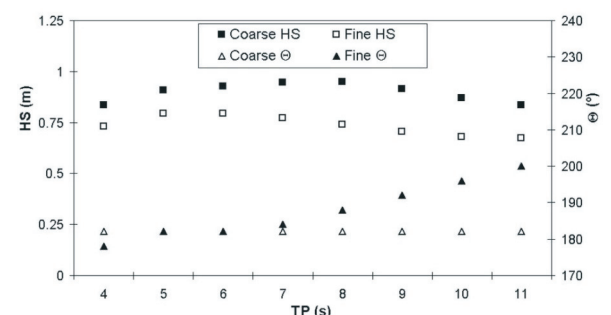


Figure 7. Differences in HS and  $\Theta$  between the two SWAN grid runs. Sea states at SINES 1D with HS = 1 m and  $\Theta$  = 180°.

In fact, this type of model operation and the use of two nested grids and of the transfer matrix provided some insight on the most adequate methodology to process future wave data that may be received from the SINES 1D wave buoy. This way, whenever the wave buoy broadcasts new measurements, a quick processing of these data to estimate the sea state at P may consist of using the parameters defined for that sea state in the interpolation matrix built for this study. This kind of information close to the breakwater can be used to issue warnings on the safety of both the structure and the port operations. A more elaborate, and time consuming, procedure will include the input of the data from the wave buoy into the SWAN model with the spatial grids the coarse and the nested grid - used for this study. Ideally the characterization of the energy distribution of frequency and direction ranges should be available. Then, instead of the JONSWAP model for the definition of the sea state at the buoy location one could use a more accurate description of that sea state and this would produce a better prediction of the sea state in front of the west breakwater. With this prediction one may update the wave regimes, the observed and, eventually, the extreme wave regimes, in front of that structure and this will be of use to evaluate the actions on the structure and hence to the structure's diagnosis, which the major aim of the MEDIRES project.

### ACKNOWLEDGEMENTS

The authors would like to acknowledge the financial support

of the study "Stochastic Modeling of Sea Waves" of the project "Modeling of Sea waves and Currents" from LNEC's own research plan for 2001-2004. The MEDIRES project has the financial support of Portuguese government funds and the European Fund for Regional Development.

### LITERATURE CITED

- BOOIJ, N.R.; HOLTHUIJSEN, L.H. and RIS, R.C., 1996. The SWAN wave model for shallow water. *ICCE'96*, Orlando, 668-676.
- COLI, A.B.; SANTOS, J.A.; FORTES, C.J.; CAPITÃO, R. and CARVALHO, M.M., 2002. Metodologia de propagação de regimes de agitação marítima do largo para a costa: análises dos modelos BACKTRACK-REFSPEC e SWAN. *6º Congresso da Água*, Oporto, Portugal.
- COSTA, M.S., 1988-1995. Tratamento de dados de agitação marítima. Sines. *Series of technical reports from May 1988 to December 1995*. Instituto Hidrográfico, Lisbon, Portugal.
- MELBY, J.A. and KOBAYASHI, N., 1998. Progression and variability of damage on rubble-mound breakwaters. *J. Waterway, Port, Coast and Ocean Engineering*, ASCE, 124(6), 286-294.
- SOARES, C.G.; NOLASCO, M.C. and MENDES, P., 1992. Probabilidade de ocorrência de estados de mar combinados na Costa Portuguesa. In: SOARES, C.G. (ed.), *A engenharia naval em Portugal*, vol. IX, Lisbon, Portugal, pp.13.1-13.32.